Electronic transition energy E ii for an isolated (n , m) single-wall carbon nanotube obtained by anti-Stokes/Stokes resonant Raman intensity ratio

PHYSICAL REVIEW B, VOLUME 63, 241404(R)

Electronic transition energy E_{ii} for an isolated (n,m) single-wall carbon nanotube obtained by anti-Stokes/Stokes resonant Raman intensity ratio

A. G. Souza Filho,[1,2] A. Jorio,[1] J. H. Hafner,[3] C. M. Lieber,[3] R. Saito,[4] M. A. Pimenta,[5] G. Dresselhaus,[6] and M. S. Dresselhaus[1,7]

[1]*Department of Physics, Massachusetts Institute of Technology, Cambridge, Massachusetts 02139*

[2]*Departamento de Física, Universidade Federal do Ceará, Fortaleza, Ceará 60455-760 Brazil*

[3]*Department of Chemistry, Harvard University, Cambridge, Massachusetts 02138*

[4]*Department of Electronic-Engineering, University of Electro-Communications, Tokyo, Japan, 182-8585*

[5] *Departamento de Física, Universidade Federal de Minas Gerais, Belo Horizonte, Minas Gerais, 30123-970 Brazil*

[6]*Francis Bitter Magnet Laboratory, Massachusetts Institute of Technology, Cambridge, Massachusetts 02139*

[7]*Department of Electrical Engineering and Computer Science, Massachusetts Institute of Technology, Cambridge, Massachusetts 02139*

(Received 12 February 2001; revised manuscript received 6 April 2001; published 6 June 2001)

A resonant Raman study of the anti-Stokes and Stokes spectra for individual isolated single-wall carbon nanotubes is presented. The observed asymmetry between the anti-Stokes and Stokes spectra is analyzed within the framework of resonant Raman scattering theory, thereby providing a method for accurately determining the transition energy between van Hove singularities E_{ii} in the electronic density of states and unambiguously assigning the (n,m) nanotube indices. Furthermore, resonant Raman theory allows us to determine whether the resonance is with the *incident* or *scattered* photon, and to estimate the relative magnitudes of the matrix elements for the *G*-band and the radial breathing mode Raman processes.

DOI: 10.1103/PhysRevB.63.241404 PACS number(s): 73.22.−f

Carbon nanotubes have received much attention, not only for their high application potential as nanodevices, but also because they represent a unique one-dimensional (1D) system where fundamental concepts can be evaluated to achieve new physical insights.[1,2] The low dimensionality of this system leads to quantum confinement-induced van Hove singularities in the electronic density of states (DOS), which are responsible for strong resonant Raman effects.[2]

Resonant Raman scattering (RRS) has been established as a powerful technique to investigate single-wall carbon nanotubes (SWNTs), providing valuable information about the electronic DOS,[2,3] and to distinguish between metallic and semiconducting nanotubes, just by analyzing the line shape of the tangential *G*-band profile (around 1600 cm^{-1}).[4–6] Furthermore, the anti-Stokes spectra of individual isolated SWNTs can be compared with their corresponding Stokes spectra, and the experimental results exhibit unique features when compared with other systems. Brown *et al.*[7] reported a systematic study of the anti-Stokes (AS) and Stokes (S) spectra for SWNT bundles with emphasis on the *G*-band, where the laser excitation energy E_{laser} was especially chosen to show large asymmetries between the anti-Stokes and Stokes spectra. The most dramatic asymmetries were observed when metallic nanotubes in the bundle were resonant in the anti-Stokes spectrum and semiconducting tubes were resonant in the Stokes spectrum (or vice versa) at the same incident photon energy E_{laser}. Large asymmetries between the anti-Stokes and Stokes spectra for SWNTs were also reported for the radial breathing mode (RBM), and these asymmetries were attributed[8] to the coexistence of resonant and nonresonant Raman scattering processes for SWNTs with different diameters d_t. Both of these investigations point to the importance of the scattered photon in the RRS process for SWNTs.

All of the above-mentioned studies were performed on SWNT bundles providing average results over many nanotubes with different chiralities. Developments in synthesis techniques for SWNTs now make it possible to produce isolated SWNTs,[9] and to observe resonant Raman spectra from one isolated SWNT,[10] thus improving our understanding of the physical basis for RRS effects in 1D systems. With a single laser line E_{laser}, it is possible to assign the (n,m) structure of each isolated SWNT in resonance with E_{laser} by measuring the RBM frequency (ω_{RBM}).[10] Such an assignment is limited by the spectrometer resolution in the case of two different SWNTs with diameters very close to each other, since $\omega_{\text{RBM}} = \alpha/d_t$.[10] Also, by continuously varying E_{laser}, the resonant window and the joint density of states (JDOS) profile of one isolated SWNT can be determined.[11]

We here present a systematic study of the anti-Stokes and Stokes spectra of *isolated* SWNTs, building on previous work,[9–11] and using a sample with a low density of nanotubes per laser spot. By using these experimental results based on a single laser line and resonant Raman theory, we can accurately determine the transition energies E_{ii} between van Hove singularities in the valence and conduction bands, leading to a more reliable determination of (n,m) than can be obtained just from ω_{RBM} in the Stokes spectrum, if there is more than one nanotube with almost the same d_t value.[10] We use resonant Raman theory to determine whether the resonance for a SWNT is with the *incident* or *scattered* photon, and to estimate the ratio between the Raman matrix elements for the RBM and *G*-band features.

Isolated SWNTs were prepared by a chemical vapor deposition (CVD) method on an oxidized Si substrate containing Fe nanoparticle catalysts. The sample was characterized by atomic force microscopy (AFM), and a low SWNT

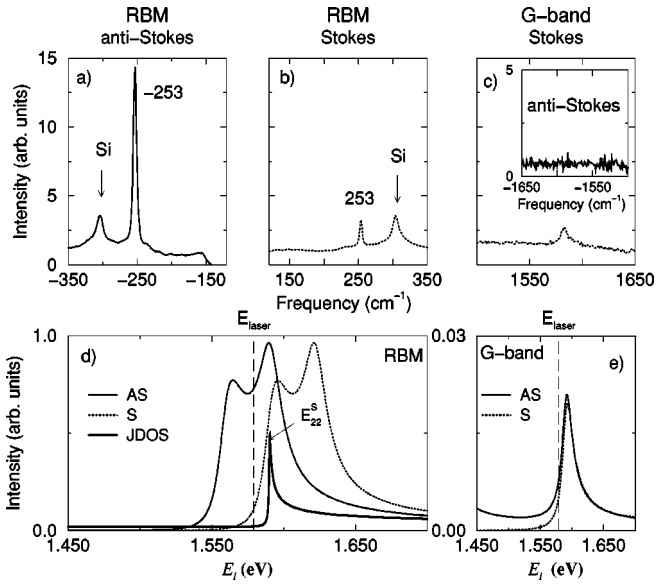

FIG. 1. (a), (b), and (c) resonant anti-Stokes and Stokes Raman spectra of a (12,1) SWNT (as identified in this work) on a Si/SiO_2 substrate, using $E_{laser}=1.579$ eV (758 nm) (vertical dashed line). The peak at 303 cm^{-1} comes from the Si substrate. The RBM frequencies are displayed in cm^{-1}. (d) Predicted joint density of states (heavy line) and resonant windows for RBM in the anti-Stokes (solid line) and Stokes (dotted line) process for the SWNT in spectra (a)–(c). (e) Resonant windows for the *G*-band in the anti-Stokes (solid line) and Stokes (dotted line) process for the SWNT in spectra (a)–(c) in the region where the resonance is with the incident photon.

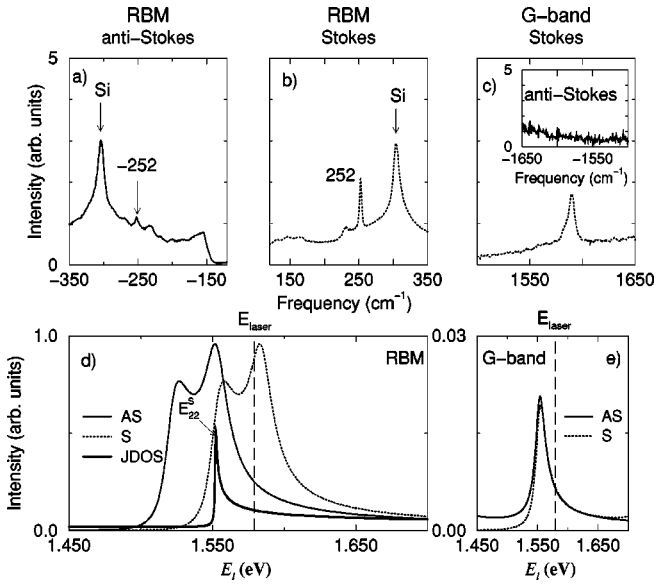

FIG. 2. (a), (b), (c), (d), and (e) are the same as in Fig. 1, except that the data here are for the (11,3) SWNT.

density (3 ± 2 isolated SWNTs per μm^2) was found. The probability of finding two tubes resonant with the same E_{laser} in one laser spot on this very low density sample is about (1/100). From 40 SWNTs observed by AFM, the diameter distribution of the sample was fit by a Gaussian distribution with $d_t=1.80\pm0.62$ nm and an accuracy better than ±0.2 nm. Raman spectra were taken with a Kaiser Optical Systems, Inc. Hololab 5000R; Modular research micro-Raman spectrograph (spot size of 1 μm diameter). The 785 nm ($E_{laser}=1.579$ eV) excitation from a Ti:sapphire laser was used. The laser power impinging on the sample surface was about 25 mW. To account for the SWNT temperature T in the data analysis, the measured anti-Stokes intensity was multiplied by $[n(E)+1]/n(E)$, and the resulting normalized anti-Stokes spectra I_{AS} are plotted, where $n(E)=1/[\exp(E/k_BT)-1]$ is the Bose-Einstein thermal factor, E is the energy, and k_BT the thermal energy. A temperature $T=300$ K was found for both the 303 cm^{-1} (see Figs. 1–3) and 521 cm^{-1} features in the Si substrate spectrum (not shown). Furthermore, no significant heating of the SWNTs was observed. The temperature coefficient of the frequency of the *G*-band and the RBM mode in SWNTs is ~-0.038 and -0.013 cm^{-1}/K, respectively.[12] Neither the RBM nor the *G*-band exhibit a frequency shift by changes of the laser power from 1 mW to 35 mW. The *G*-band, which has a well-known frequency value (~1592 cm^{-1}) and a larger temperature coefficient, does not appear to be downshifted in our single nanotube measurements. The fact that the isolated nanotubes do not exhibit significant heating is another indication of the unusually high thermal conductivity of carbon nanotubes and the good thermal contact to the substrate.[13]

Figures 1(a)–1(c) show both Stokes and anti-Stokes spectra for the RBM and the *G*-band for one isolated SWNT. Here the normalized anti-Stokes intensity at $\omega_{RBM}=253$ cm^{-1} is much larger than the Stokes intensity. This asymmetry in intensity between the anti-Stokes and Stokes

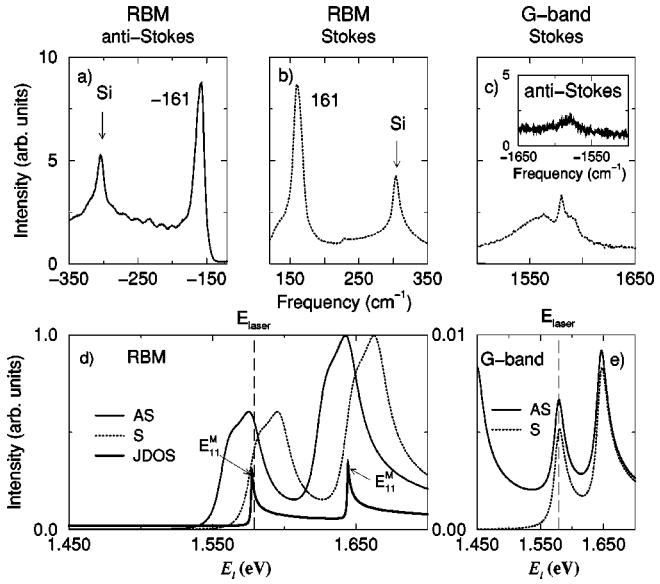

FIG. 3. (a), (b), (c), (d), and (e) are the same as in Figs. 1 and 2, except that the data here are for a (14,8) metallic SWNT. The van Hove singularity at 1.642 eV in (d) is too far from E_{laser} and too far from $E_{laser}\pm E_G$ to contribute significantly to the spectra shown, where E_G is the G-band phonon energy. The tail in (e) for I_{AS} is due to resonance with the scattered photon ($E_{ii}^M-E_G=1.382$ eV) which comes from the van Hove singularity at 1.642 eV and $E_G=0.197$ eV.

RBM spectra can be quantitatively analyzed by using resonant Raman theory, and the resonant window $I(E_l)$ for both the anti-Stokes and Stokes spectra from one isolated tube is calculated using the equation[11]

$$I(E_l)=\int \left| \frac{Mg(E)}{(E_l-E-i\Gamma_r)(E_l\pm E_{ph}-E-i\Gamma_r)} \right|^2 dE, \quad (1)$$

where E_l represents all possible laser energies, E_{ph} is the phonon energy, $+(-)$ applies to anti-Stokes (Stokes) scattering, Γ_r is associated with the lifetime of electronic states in the resonant process, M is the matrix element which accounts for radiation and photon-phonon coupling (absorption and emission) and the coupling between electrons and phonons, and $g(E)$ is the joint density of electronic states (JDOS) as described in Ref. 11. Since $I(E_l)$ is large only near resonance, we assume that M is independent of E and depends only on the phonon feature. By taking the parameters $\Gamma_J=0.5$ meV (Γ_J is a measure of finite size effects on the width of the JDOS singularities[11] for the E_{ii} electronic transition), and $\Gamma_r=8.0$ meV, determined experimentally for a specific isolated SWNT,[11] we plot the resonant window $I(E_l)$ for a given E_{ii} and E_{ph}. Figure 1(d) shows both the anti-Stokes (solid line) and Stokes (dotted line) RBM resonant windows for $\omega_{\mathrm{RBM}}=253$ cm^{-1} ($E_{ph}=0.031$ eV) and $E_{ii}=1.587$ eV. The E_{ii} value is chosen to satisfy the observed integrated intensity ratio $I_{\mathrm{AS}}/I_{\mathrm{S}}=6.96$ for $E_l=E_{\mathrm{laser}}=1.579$ eV [vertical dashed line in Fig. 1(d)]. Thus, using resonant Raman scattering theory,[11] and the $I_{\mathrm{AS}}/I_{\mathrm{S}}$ ratio, the E_{ii} value can be determined with a precision better than 10 meV. The JDOS profile (heavy line) is also plotted in Fig. 1(d).

The opposite situation, where $I_{\mathrm{AS}}/I_{\mathrm{S}}<1$, is now analyzed. Figures 2(a)–2(c) show both Stokes and anti-Stokes spectra for the RBM and G-band for another isolated SWNT. We observe in Figs. 2(a) and 2(b) that $I_{\mathrm{S}}>I_{\mathrm{AS}}$ at $\omega_{\mathrm{RBM}}=252$ cm^{-1}. Applying a similar analysis as described for Fig. 1, we determine $E_{ii}=1.554$ eV for the SWNT depicted in Figs. 2(a)–2(c). Therefore, the asymmetries observed in I_{AS} and I_{S} for the spectra in Figs. 1(a)–1(b), and 2(a)–2(b) can be understood by observing the resonant windows for these tubes. For the spectra in Figs. 1(a) and 1(b), the I_{AS} intensity comes from both *incident* (E_{laser}) and *scattered* ($E_{\mathrm{laser}}+E_{ph}$) photon contributions, while the I_{S} intensity comes only from resonance with the *incident* photon. In contrast, for the spectra in Figs. 2(a) and 2(b), the I_{AS} intensity comes from resonance with the *incident* photon and I_{S} has resonant contributions from both *incident* and *scattered* ($E_{\mathrm{laser}}-E_{ph}$) photons. We emphasize that $I_{\mathrm{AS}}/I_{\mathrm{S}}$ for a given SWNT is almost independent of experimental factors that affect the absolute intensities I_{AS} and I_{S}, such as the focus condition and the nanotube length.

In contrast to the striking asymmetries between the anti-Stokes and Stokes RBM spectra discussed above is the situation where the van Hove singularity E_{ii} is very close to E_{laser}, so that $I_{\mathrm{AS}}\approx I_{\mathrm{S}}$, and the resonance is with the *incident* photon. We show in Fig. 3 both the anti-Stokes and Stokes RBM (a and b) and G-band (c and inset) spectra for a third isolated SWNT taken at $E_{\mathrm{laser}}=1.579$ eV. Here the observed I_{S} and I_{AS} at $\omega_{\mathrm{RBM}}=161$ cm^{-1} are almost equal, with $I_{\mathrm{AS}}/I_{\mathrm{S}}=1.13$, implying that the resonance occurs very close to the electronic transition $E_{ii}\approx E_{\mathrm{laser}}$. The strong intensity of the RBM features observed in Figs. 1–3 can be explained by the double resonance Raman process.[17] The denominator in Eq. 1 has two resonant terms [$E_l=E_{ii}$ (*incident* photon) and $E_l=E_{ii}\pm E_{ph}$ (*scattered* photon)] that nearly go to zero *quasi* simultaneously because E_{RBM} is small (0.019–0.032 eV).

According to a recent resonant Raman study of one isolated nanotube,[10] the RBM frequency (ω_{RBM}) and nanotube diameter (d_t) are related by $\omega_{\mathrm{RBM}}=\alpha/d_t$, ($\alpha=248$ cm^{-1} nm), making possible the (n,m) identification of this SWNT considering only the observed ω_{RBM} and I_{RBM}. Based on this method,[10] the SWNT whose spectra are in Fig. 3 is identified as the metallic (14,8) SWNT.[10] The trigonal warping effect splits the van Hove singularities E_{11}^M for metallic nanotubes[15,16] and for the (14,8) SWNT, the values for E_{11}^M are 1.577 and 1.642 eV, as we can see in the JDOS (heavy line) profile, plotted in Fig. 3(d). It is predicted for the metallic (14,8) tube, that $I_{\mathrm{AS}}/I_{\mathrm{S}}=1.20$, which is in excellent agreement with the experimental measurement of $I_{\mathrm{AS}}/I_{\mathrm{S}}=1.13$, thereby confirming the (14,8) assignment.

However, in the case of the small diameter SWNTs in Figs. 1 and 2 with $\omega_{\mathrm{RBM}}=252$ and 253 cm^{-1}, the (n,m) assignment cannot be done unambiguously, based only on the ω_{RBM} values. This difference in frequency is smaller than the standard spectrometer accuracy (~ 2 cm^{-1}) and both of these signals could be assigned as coming from the same (n,m) SWNT if we consider only the Stokes spectra. However, by considering the $I_{\mathrm{AS}}/I_{\mathrm{S}}$ ratio at E_{laser}, we can clearly assign the proper (n,m) indices to these tubes as follows. The experimental determinations of E_{ii} as 1.587 and 1.554 eV, respectively, for tubes with $\omega_{\mathrm{RBM}}=253$ and 252 cm^{-1} are very close to those found by direct calculation for (12,1) and (11,3) nanotubes,[1,14] which are $E_{ii}=1.585$ and 1.564 eV, respectively (here we used $\gamma_0=2.89$ eV, in good agreement with previous work.[3,10,11]). It is predicted theoretically that $I_{\mathrm{AS}}/I_{\mathrm{S}}>1$ and <1 at E_{laser} for the (12,1) and (11,3) tubes, respectively, thereby clearly identifying $\omega_{\mathrm{RBM}}=253$ cm^{-1} with the (12,1) tube and $\omega_{\mathrm{RBM}}=252$ cm^{-1} with the (11,3) tube. By considering $I_{\mathrm{AS}}/I_{\mathrm{S}}$ at E_{laser}, we are thus able to eliminate ambiguities in the (n,m) assignments as discussed above. This result points out the importance of the $I_{\mathrm{AS}}/I_{\mathrm{S}}$ intensity ratio to give a high degree of certainty for the (n,m) assignments of two or more isolated SWNTs with similar d_t values. Such a situation occurs frequently for RBM's observed by the resonance of E_{laser} with E_{ii} for larger diameter SWNTs.

Finally, we use resonant Raman theory to estimate the ratio between the matrix elements associated with the G-band (M_G) and the RBM (M_{RBM}) for the nanotubes in Figs. 1–3. By comparing the predicted $I_G|M_{\mathrm{RBM}}|^2/I_{\mathrm{RBM}}|M_G|^2$ and the observed integrated intensity ratio I_G/I_{RBM} for $E_l=E_{\mathrm{laser}}=1.579$ eV, we made an estimation of M_G/M_{RBM} for the three SWNTs discussed in this work, and we found $M_G/M_{\mathrm{RBM}}=5.0$, 10.0, and 2.5 for the (12,1), (11,3), and (14,8) tubes, respectively. Since the two

semiconducting tubes (12,1) and (11,3) have almost the same diameter, these results for the M_G/M_{RBM} values may indicate a possible chirality dependence of M_G/M_{RBM}, since (12,1) and (11,3) have chiral angle $\theta=4°$ and 11°, respectively. For the metallic (14,8) SWNT, the M_G/M_{RBM} value is smaller than for the semiconducting tubes, indicating that the magnitude of the *electron-phonon* coupling for metallic and semiconducting SWNTs may be different. This is reasonable because of the *screening* of charge by the conduction electrons in metallic nanotubes, which affects the RBM and *G*-band vibrations in different ways. The analysis performed here suggests a new scenario in resonant Raman scattering where the evaluation of the intensity for all Raman spectral features is possible, and by varying E_{laser}, more detailed information about the resonant process can be obtained as a function of nanotube diameter and chirality.

The analysis of the *G*-band anti-Stokes spectra also gives valuable information. The anti-Stokes spectra can be observed only if the first excited phonon state is populated. Since its intensity compared with the Stokes spectra is proportional to $\exp[-E_{ph}/kT]$, the anti-Stokes *G*-band intensity at 300 K is expected to be very small, unless the *incident* (E_{laser}) or *scattered* ($E_{\mathrm{laser}}+0.197=1.776$ eV) photon is very close to an electronic transition E_{ii} between van Hove singularities, where the Raman signal is strongly enhanced. The experimental observation of the anti-Stokes *G*-band for the (14,8) isolated SWNT [see inset in Fig. 3(c)] indicates that this tube is in strong resonance with the *incident* photon [see Fig. 3(e)], consistent with our interpretation of the RBM spectra, and that the *G*-band and the RBM features come from the same tube. The corresponding *G*-band I_{AS} for the (12,1) and (11,3) nanotubes, where the RBM is not exactly resonant with the *incident* photon, is too low to be seen in the anti-Stokes *G*-band spectra. Theory predicts that E_{laser} intersects the *G*-band resonant window only in the wings [see Figs. 1(e) and 2(e)], where I_{AS} (solid lines) is expected to be low and the signal is below the noise level, in agreement with its absence experimentally even after normalization by $\exp[-E_{ph}/kT]$ [see insets to Figs. 1(c) and 2(c)].

In summary, a resonant Raman scattering study of anti-Stokes and Stokes spectra of isolated single-wall nanotubes is reported here. The $I_{\mathrm{AS}}/I_{\mathrm{S}}$ intensity ratio for the RBM is shown to depend sensitively on $E_{ii}-E_{\mathrm{laser}}$. Therefore, we can use the RBM $I_{\mathrm{AS}}/I_{\mathrm{S}}$ ratio at E_{laser} to determine E_{ii} accurately and whether the resonance is with the *incident* or *scattered* photon, and to resolve ambiguities in the (n,m) assignment between two or more likely candidates with similar d_t values. We also show how resonant Raman theory could be used to estimate the ratio between the *G*-band and the RBM matrix elements (M_G/M_{RBM}), which is important for discussing the *electron-phonon* coupling in semiconducting and metallic SWNTs. The analysis performed in this work demonstrates a significant advance in understanding the resonant Raman process in SWNTs, definitively establishing resonant Raman spectroscopy as a powerful technique to characterize *one single* carbon nanotube.

A.G.S.F. and A.J. thank the Brazilian agencies CAPES and CNPq, respectively, for financial support. This work made use of the MRSEC Shared Facilities at MIT, supported by the National Science Foundation under Grant No. DMR-9400334 and NSF Laser facility Grant No. 97-08265-CHE. The MIT authors acknowledge support under NSF Grants Nos. DMR 98-04734, INT 98-15744 and INT 00-00408. R.S. acknowledges a Grant-in-Aid (No. 11165216 and 13440091) from the Ministry of Education, Japan.

[1] R. Saito, G. Dresselhaus, and M. S. Dresselhaus, in *Physical Properties of Carbon Nanotubes* (Imperial College Press, London, 1998).

[2] M. S. Dresselhaus and P. C. Eklund, Adv. Phys. **49**, 705 (2000), and references therein.

[3] M. Milnera, J. Kürti, M. Hulman, and H. Kuzmany, Phys. Rev. Lett. **84**, 1324 (2000).

[4] M. A. Pimenta, A. Marucci, S. Empedocles, M. Bawendi, E. B. Hanlon, A. M. Rao, P. C. Eklund, R. E. Smalley, G. Dresselhaus, and M. S. Dresselhaus, Phys. Rev. B **58**, R16 016 (1998).

[5] S. D. M. Brown, A. Jorio, P. Corio, M. S. Dresselhaus, G. Dresselhaus, R. Saito, and K. Kneipp, Phys. Rev. B **63**, 155414 (2001).

[6] P. M. Rafailov, H. Jantoliak, and C. Thomsen, Phys. Rev. B **61**, 16 179 (2000).

[7] S. D. M. Brown, P. Corio, A. Marucci, M. S. Dresselhaus, M. A. Pimenta, and K. Kneipp, Phys. Rev. B **61**, R5137 (2000).

[8] P. H. Tan, Y. Tang, C. Y. Hu, F. Li, Y. L. Wei, and H. M. Cheng, Phys. Rev. B **62**, 5186 (2000).

[9] J. H. Hafner, C. L. Cheung, T. H. Oosterkamp, and C. M. Lieber, J. Phys. Chem. B **105**, 743 (2001).

[10] A. Jorio, R. Saito, J. H. Hafner, C. M. Lieber, M. Hunter, T. McClure, G. Dresselhaus, and M. S. Dresselhaus, Phys. Rev. Lett. **86**, 1118 (2001).

[11] A. Jorio, A. G. Souza Filho, G. Dresselhaus, M. S. Dresselhaus, J. H. Hafner, C. M. Lieber, R. Saito, F. Matinaga, M. S. S. Dantas, and M. A. Pimenta, Phys. Rev. B (to be published).

[12] H. D. Li *et al.*, Appl. Phys. Lett. **76**, 2053 (2000).

[13] S. Berber, Y.-K. Kwon, and D. Tománek, Phys. Rev. Lett. **84**, 4613 (2000).

[14] H. Kataura, Y. Kumazawa, Y. Maniwa, I. Umezu, S. Susuki, Y. Ohtsuka, and Y. Achiba, Synth. Met. **103**, 2555 (1999).

[15] R. Saito, G. Dresselhaus, and M. S. Dresselhaus, Phys. Rev. B **61**, 2981 (2000).

[16] P. Kim, T. W. Odom, J.-H. Huang, and C. M. Lieber, Phys. Rev. Lett. **82**, 1225 (1999).

[17] R. M. Martin and L. M. Falicov, in *Light Scattering in Solids I*, edited by M. Cardona, Topics in Applied Physics Vol. 8 (Springer, Berlin, 1975), p. 79.